A Hydraulic Model Is Compatible with Rapid Changes in Leaf Elongation under Fluctuating Evaporative Demand and Soil Water Status[1][C][W][OPEN]

Cecilio F. Caldeira, Mickael Bosio, Boris Parent, Linda Jeanguenin, François Chaumont, and François Tardieu*

INRA, Unité Mixte de Recherche 759 Laboratoire d'Ecophysiologie des Plantes sous Stress Environnementaux, F–34060 Montpellier, France (C.F.C., B.P., F.T.); Biogemma, 63028 Clermont-Ferrand cedex 2, France (M.B.); and Institut des Sciences de la Vie, Université Catholique de Louvain, B–1348 Louvain-la-Neuve, Belgium (L.J., F.C.)

Plants are constantly facing rapid changes in evaporative demand and soil water content, which affect their water status and growth. In apparent contradiction to a hydraulic hypothesis, leaf elongation rate (LER) declined in the morning and recovered upon soil rehydration considerably quicker than transpiration rate and leaf water potential (typical half-times of 30 min versus 1–2 h). The morning decline of LER began at very low light and transpiration and closely followed the stomatal opening of leaves receiving direct light, which represent a small fraction of leaf area. A simulation model in maize (*Zea mays*) suggests that these findings are still compatible with a hydraulic hypothesis. The small water flux linked to stomatal aperture would be sufficient to decrease water potentials of the xylem and growing tissues, thereby causing a rapid decline of simulated LER, while the simulated water potential of mature tissues declines more slowly due to a high hydraulic capacitance. The model also captured growth patterns in the evening or upon soil rehydration. Changes in plant hydraulic conductance partly counteracted those of transpiration. Root hydraulic conductivity increased continuously in the morning, consistent with the transcript abundance of *Zea maize Plasma Membrane Intrinsic Protein* aquaporins. Transgenic lines underproducing abscisic acid, with lower hydraulic conductivity and higher stomatal conductance, had a LER declining more rapidly than wild-type plants. Whole-genome transcriptome and phosphoproteome analyses suggested that the hydraulic processes proposed here might be associated with other rapidly occurring mechanisms. Overall, the mechanisms and model presented here may be an essential component of drought tolerance in naturally fluctuating evaporative demand and soil moisture.

In natural conditions, evaporative demand varies over minutes to hours with changes in light, temperature, and dew point. Soil water status varies over hours to days with soil evaporation, plant water uptake, and rainfall. Hence, water movements in the plant are constantly facing boundary conditions that change from low to high offer and demand, leading to rapid oscillations of leaf water status and growth (Hsiao et al., 1970; Ben Haj Salah and Tardieu, 1997; Walter et al., 2009). These rapid changes are artificially avoided in most in-depth analyses of plant growth, metabolism, and omics, viewed as requiring stable environmental conditions for comparisons between experiments and days. For instance, Baerenfaller et al. (2012) analyzed plant adaptation to stable and moderate water deficits provided by the PHENOPSIS phenotyping platform (Granier et al., 2006). A surprising result was that a limited number of transcripts and proteins changed in abundance with water deficit. It differed from cases with rapidly imposed water stresses, for which the timing and protocol of stress imposition plays a major role in gene expression (Bray, 1997). This suggests that essential processes may occur during transitions of the water status of soil or air rather than during periods with stable conditions. Leaf elongation rate (LER) is very sensitive to both soil water status and evaporative demand in most monocotyledons, thereby varying dramatically during the day (Hsiao et al., 1970; Ben Haj Salah and Tardieu, 1997; Munns et al., 2000). These transitions represent a large proportion of the lifespan of plants in natural conditions because of clouds, daily alternations of light, and rain episodes, so plant behavior during them may be a major determinant for growth response to water deficit and of its genetic variability.

Rapid fluctuations of LER are associated, in monocotyledons, with local events in the growth zone located

[1] This work was supported by the European Union (project no. FP7–244374 [Drought Tolerant Yielding Plants (DROPS)]); the Agence Nationale de la Recherche (ANR)–08–GENM–003 project; the Région Languedoc-Roussillon; the Interuniversity Attraction Poles Programme, Belgian Science Policy; and the Belgian French community Action de Recherche Concertée (ARC)11/16–036 project.

* Address correspondence to françois.tardieu@supagro.inra.fr.

The author responsible for distribution of materials integral to the findings presented in this article in accordance with the policy described in the Instructions for Authors (www.plantphysiol.org) is: François Tardieu (francois.tardieu@supagro.inra.fr).

[C] Some figures in this article are displayed in color online but in black and white in the print edition.

[W] The online version of this article contains Web-only data.

[OPEN] Articles can be viewed online without a subscription.

www.plantphysiol.org/cgi/doi/10.1104/pp.113.228379

in a few-centimeter-long region at the base of the leaf (Schnyder and Nelson, 1988; Ben Haj Salah and Tardieu, 1997). Several mechanisms are potential candidates for these fluctuations. (1) Hydraulic processes are associated with expansive growth, with simultaneous changes in cell turgor and LER upon rapid variations of hydraulic conductivity (Ehlert et al., 2009) and/or with changes in the gradient of water potential between the xylem and growing tissues (Tang and Boyer, 2002, 2008). (2) Cell wall mechanical properties are affected by water deficit in the growth zone with the involvement of abscisic acid (ABA), potentially combined with other hormones or apoplastic pH (Tardieu et al., 2010). The abundance of expansin transcripts decreases with water deficit in the growth zones of maize (*Zea mays*) leaves (Muller et al., 2007), while cell wall peroxidase activity and caffeate *O*-methyltransferase abundance increase (Bacon et al., 1997; Vincent et al., 2005; Zhu et al., 2007). (3) Cell division rate strongly decreases in the maize leaf under water deficit via the effect of p34CDC2 kinase that blocks cells in the G1 phase (Granier et al., 2000).

These mechanisms have markedly different time constants. A whole cell cycle takes about 1 d (Granier and Tardieu, 1998; Granier et al., 2000), changes in cell wall properties take minutes to hours (Chazen and Neumann, 1994), and hydraulic processes occur over seconds to minutes (Ye and Steudle, 2006; Tang and Boyer, 2008; Parent et al., 2009). While analysis of time constants is a common method to identify the most likely mechanisms affecting time courses in physics (Kim et al., 2008; Knowles et al., 2009) or enzymology (Schweizer et al., 1998; Wang et al., 2007; Zheng et al., 2013), it is less common in studies of growth or of genomics applied to responses to environmental conditions. The progress of phenotyping now allows one to obtain a large number of time courses of LER, transpiration, and environmental conditions with a time step of minutes (Sadok et al., 2007), thereby making possible the use of this method.

In this study, we have analyzed time courses of maize LER and of potential mechanisms in order to identify most likely candidates for the rapid changes of LER during the transitions of evaporative demand and soil water status. This was performed at transitions between dawn and morning, between afternoon and night, and during rehydration of droughted plants. Because previous genetic analyses carried out on the same material suggested a major role for hydraulic processes (Parent et al., 2009; Tardieu et al., 2010; Welcker et al., 2011), we have focused on hydraulic measurements of water potential, hydraulic conductivity, and amount of PIP aquaporin transcripts. The proposed mechanism of elongation control during rapid changes of environmental conditions was then tested with a model. Finally, other putative controls were analyzed via a temporal series of genome-wide transcriptomes, presented in this study, and of a phosphoproteome published in a companion paper (Bonhomme et al., 2012).

RESULTS

The Decrease in LER Did Not Match with Whole-Plant Transpiration in the Early Morning

A total of 1,877 daily time courses of LER originating from 23 experiments (Supplemental Table S1) were classified into a limited number of patterns in each experiment, according to the evaporative demand and water availability measured on the considered day. Overall, the decline of LER was associated with sunrise regardless of time of day in the range of 4.5 to 7 AM; transpiration and LER followed opposite trends, with larger daily depressions on days with higher transpiration rate or under very mild water deficit (Fig. 1; Supplemental Figs. S1 and S2). However, the decrease in LER at the transition between day and night was much more rapid than that of transpiration rate, with mean half-times of 0.8 ± 0.3 and 2.3 ± 0.5 h, respectively, in the mornings of 14 experiments (Supplemental Table S1; Supplemental Fig. S3). It occurred at a time when transpiration rate was still almost negligible (5 ± 3 g m^{-2} h^{-1}) due to low values of photosynthetic photon flux density (PPFD) and vapor pressure deficit (VPD; 10 ± 3 μmol m^{-2} s^{-1} and 0.75 ± 0.2 kPa, respectively, over the whole data set). Interestingly, this was also the case on days with low evaporative demand, when LER declined rapidly in spite of a very slow increase in transpiration rate (Fig. 1, I–J). The relation between transpiration and LER was clearly nonlinear in the morning but also during recovery in the late afternoon (Supplemental Figs. S1 and S2). Hence, changes in LER might be considered as either independent of transpiration rate or extremely sensitive to it.

The Change in Whole-Leaf Water Potential Was Considerably Slower Than That in LER upon Increase in Evaporative Demand or Soil Rehydration

Leaf water potential decreased with transpiration rate over 4 h during the morning in plants grown in soil or in a hydroponic solution (soil or solution water potential, −0.15 MPa; Figs. 2 and 3), much slower than the decrease in LER. The water potential of nontranspiring leaves (covered with plastic and aluminum foil) followed the same trend, with a tendency to be lower than that of uncovered leaves in the early morning and higher during the late morning (Fig. 2B).

The recovery of LER and of leaf water potential upon rewatering was analyzed in three independent experiments with a time resolution of 5 min (Fig. 4). Plants were first grown for 8 h at a soil water potential of −0.6 ± 0.1 MPa and high evaporative demand (PPFD = 800 μmol m^{-2} s^{-1} and VPD = 3 kPa), resulting in a leaf water potential of −1.5 MPa. They were subjected at time 0 to a massive and rapid irrigation while lights were turned off and VPD was decreased to 0.8 kPa. LER did not react for 25 min and then completely recovered in 45 min. The recovery of leaf water potential was markedly slower than that of LER. After a time lapse similar to that

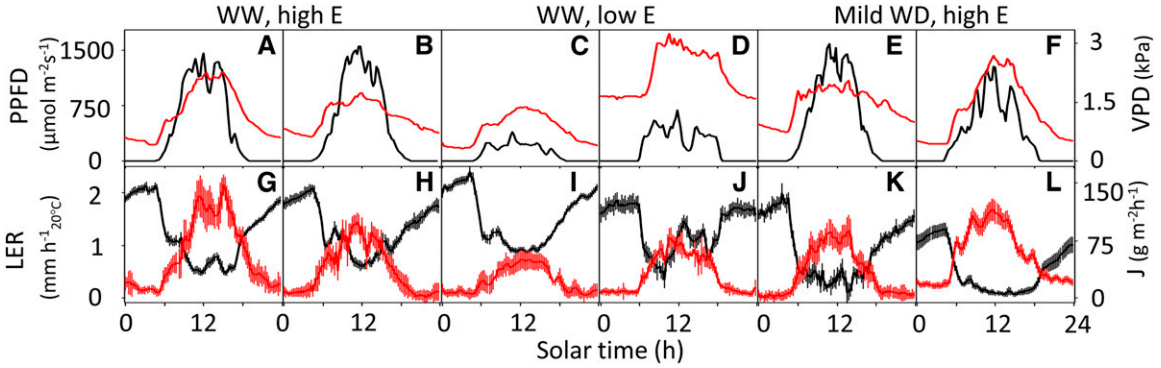

Figure 1. Daily time courses of environmental conditions, transpiration (J), and LER in six groups of experiments. A, B, G, and H, Experiments 8 and 11 (82 and 149 time courses, respectively) with well-watered plants (WW) and high evaporative demand (E). C, D, I, and J, Experiments 9 and 19 (152 and 76 time courses, respectively) with well-watered plants and low evaporative demand. E, F, K, and L, Experiments 6 and 7 (93 and 81 time courses, respectively) with very mild water deficit (WD; soil water potential of -0.15 ± 0.05 and -0.3 ± 0.05 MPa) and high evaporative demand. In A to F, red traces show air VPD, and black traces show PPFD. In G to L, red traces show plant transpiration, and black traces show LER. Line B73 was used. All time courses have a temporal definition of 15 min. Error bars indicate confidence interval at $P < 0.05$. [See online article for color version of this figure.]

of LER with no change in water potential, the time to reach 95% recovery was more than 2 h (Fig. 4).

The faster changes in LER compared with whole-leaf water potential could indicate either that LER is highly sensitive to leaf water potential in the early morning and after soil rehydration or that LER control in the morning or after rehydration is independent from whole-leaf water potential.

The Early Morning Decline of LER Was Synchronous with That of Stomatal Conductance of Illuminated Leaves

We then investigated whether the changes in LER could be linked to hydraulic variables that react faster than whole-plant transpiration or whole-leaf water potential. In the early morning, illuminated leaves represent a small proportion of leaf area (typically less than 5%), because sunbeams are nearly horizontal at this time of the day. We measured stomatal conductance in zones of the leaf area receiving either direct sunbeams or diffuse light (Fig. 5). Stomatal conductance increased very rapidly in the early morning, considerably faster than transpiration rate, which remained low because of the low evaporative demand at that time (Fig. 1). Stomatal opening was particularly rapid in leaves whose orientation allowed receiving direct light soon after sunrise, while leaves receiving only diffuse light opened stomata more slowly, consistent with the light intensity received by both categories of leaves (Fig. 5). We checked that this is not an artifact of the greenhouse or of young plants by reanalyzing results obtained with maize at flowering time for 7 d in the field (Tardieu and Davies, 1992). From 5 to 6 AM (solar time), the stomatal conductance of leaves directly exposed to sunbeams ranged from 0.2 to 0.6 mol m^{-2} s^{-1}, versus 0.03 to 0.25 mol m^{-2} s^{-1} for leaves receiving diffuse light (data not shown).

A striking result was that the morning time course of LER followed that of stomatal conductance of illuminated leaves (Fig. 5, E and F). The small increase in transpiration rate caused by the stomatal opening in a portion of leaf area under low evaporative demand, therefore, would be sufficient to cause a decrease in LER. Indeed, the relationship between LER and stomatal conductance of illuminated leaves was linear in the two studied cases. The synchronism of LER and stomatal conductance, therefore, contrasts with slower changes in leaf water potential and transpiration rate. This conclusion still held in an experiment with low evaporative demand (Fig. 3).

Manipulation of Stomatal Conductance and Hydraulic Conductivities via the Use of Transgenic Plants Underproducing/Overproducing ABA Affected the Morning Changes in LER

To determine whether the manipulation of stomatal conductance affects the daily time course of LER, we used maize transgenic plants in which ABA biosynthesis, stomatal conductance, and hydraulic conductivities were affected by manipulation of the expression of the *9-CIS-EPOXYCAROTENOID DIOXYGENASE-VIVIPAROUS14* (*NCED-VP14*) gene (Parent et al., 2009). Antisense (AS) and sense (S) plants presented (1) a lower (respectively higher) concentration of ABA in the xylem sap (7.9, 18.5, and 438 nM in AS, wild-type and S plants, respectively), (2) a lower (respectively higher) root hydraulic conductivity (0.3×10^{-7}, 0.6×10^{-7}, and 2.5×10^{-7} m s^{-1} MPa^{-1} in AS, wild-type, and S plants, respectively), consistent with differences in the expression of *ZmPIP* genes and in the amount of proteins, and (3) a higher stomatal conductance (1.25 and 0.7 times that of the wild type; Parent et al., 2009).

These transgenic lines presented marked contrasts in the time course of LER during the morning (Fig. 6), with a pattern similar to that of B73 in wild-type plants, a more rapid decline in AS plants, and a slower

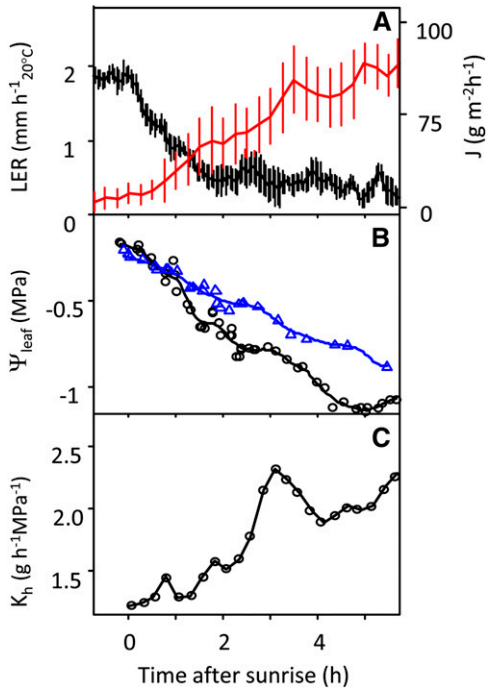

Figure 2. Time courses of LER and related variables for plants grown in soil (experiment 6, line B73). A, LER (black) and transpiration rate (J; red). B, Leaf water potential (Ψ_{leaf}) of covered (blue) and exposed (black) leaves to sunlight. C, Whole-plant hydraulic conductance (K_h). In B, trend lines are mean values estimated by kernel regression smoother (R function ksmooth). Time courses of LER and transpiration have a temporal definition of 2 min. Error bars indicate confidence interval at $P < 0.05$. [See online article for color version of this figure.]

decline in S plants. One hour after sunrise (PPFD = 60 μmol m^{-2} s^{-1}), the LER of AS, wild-type, and S plants were reduced to 30%, 50%, and 80% of night values, respectively. In addition, an experiment similar to that presented in Figure 4 (Fig. 6 in Parent et al., 2009) showed that the recovery of LER was quicker in S than in wild-type plants, with the opposite trend in AS plants. Hence, the behavior of lines with contrasting ABA synthesis was consistent with a strong implication of hydraulic conductivity and/or of stomatal conductance in the time course of LER upon changes in soil water status or evaporative demand.

Root Hydraulic Conductivity and Transcript Abundance of ZmPIPs Increased Together with the LER Decline in the Early Morning

Root hydraulic conductivity measured in a hydroponic experiment was low in the night and remained at low values for more than 1 h after sunrise (Fig. 3C). It increased steadily during the morning, with maximum values 3.0 h after sunrise. The hydraulic conductance calculated at the whole-plant level in the experiment with plants grown in soil followed a similar pattern, with slow changes in the early morning and a steady increase during the late morning (Fig. 2C).

Tissue samples were collected in roots and in the leaf elongating zone of line B73 30 min before sunrise (0 h) and 1, 2, and 6 h after it. In roots, *ZmPIP* transcripts increased markedly 1 h after sunrise, stayed at high values during the second hour, and decreased afterward (Fig. 7). This tendency was significant for three *ZmPIP* genes (*ZmPIP1;6*, *ZmPIP2;3*, and *ZmPIP2;6*), whose expression increased more than 2-fold between 0 and 1 h. Higher transcript abundances were kept during the second hour for these three genes. Four genes belonging to the PIP1 group and three to the PIP2 group had expression levels that increased 2 h after sunrise. The transcript levels of all *ZmPIP*s were reduced at 6 h after sunrise. Conversely, samples in the leaf elongating zone did not show any consistent difference in the time courses of *ZmPIP* RNA abundance during the morning (Supplemental Fig. S4).

A Simulation Model Reproduced the Observed Phenotypes Provided That Xylem Water Potential Was Partly Decoupled from Whole-Leaf Water Potential

A classical simulation model of leaf expansion would consider LER as depending directly on whole-plant transpiration and leaf water potential. The above paragraphs show that this model cannot fit with the observed phenotype. An alternative model could consist

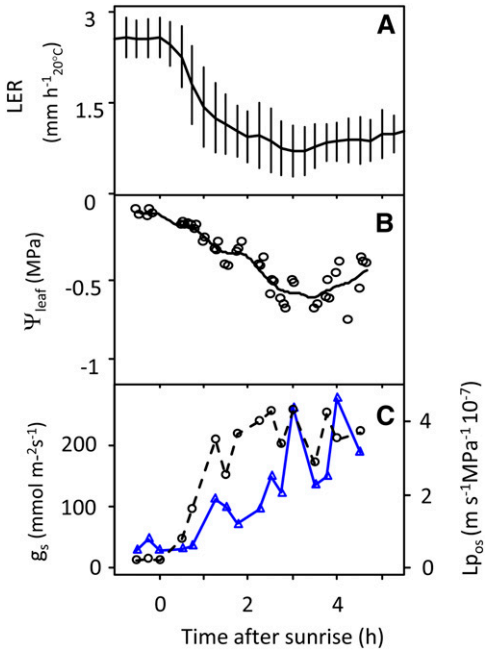

Figure 3. Time courses of LER and related variables for plants grown in hydroponics (experiment 5, line B73). A, LER. B, Leaf water potential (Ψ_{leaf}) of leaves exposed to light. C, Stomatal conductance (g_s; circles and dotted line) and root hydraulic conductivity (Lp_{os}; triangles and solid line in blue). In B, trend lines are mean values estimated by kernel regression smoother (R function ksmooth). Error bars indicate confidence interval at $P < 0.05$. [See online article for color version of this figure.]

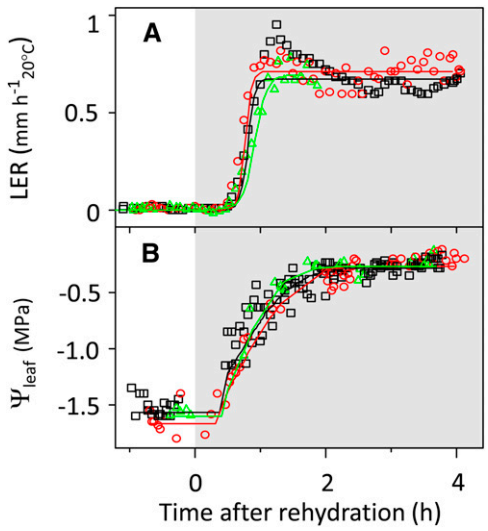

Figure 4. Time courses of the recoveries of LER and leaf water potential (Ψ_{leaf}) during soil rehydration in three independent experiments (experiments 2–4, line B73). A, Mean values of LER measured every 5 min in six to 10 plants. B, Ψ_{leaf} of uncovered leaves. Plants were watered at time 0 while lights were turned off, and VPD was set to 0.8 kPa (shaded area). Each color represents one experiment. [See online article for color version of this figure.]

in considering that LER is not associated with plant hydraulics and involves other mechanisms, such as cell wall properties associated with the circadian clock. However, we tested if a hydraulic approach could still account for the observed data, by using a model considering that LER is linked to xylem water potential, which reacts rapidly to changes in stomatal conductance or in water supply to roots, while whole-leaf water potential reacts more slowly because leaf water volume acts as a large capacitance.

The main feature of this model is a dual pathway of the xylem water flux, either toward the sites of evaporation or to the mature cells, whose water potential is that measured with a pressure chamber (Fig. 8; for a full description, see "Materials and Methods"). In this model, water flows between compartments following gradients of water potential from soil (Ψ_{soil}) to roots (Ψ_r), xylem (Ψ_{xyl}), and bundle sheaths (Ψ_{bundle}). The flux at bundle sheaths either contributes to transpiration or is diverted to mature leaf cells (having a water potential, Ψ_{cell}, and a capacitance), depending on the direction of the gradient of water potential between bundle sheaths and mature cells. R_p summarizes the resistances of root tissues, plant xylem and leaf protoxylem. It is assumed to change with time of day, consistent with Figures 2C and 3C. R_{xl} is the resistance between the xylem and bundle sheaths, and R_c is the resistance from bundle sheaths to mature leaf cells, also supposed to depend on time of day. The model of stomatal control, biosynthesis of ABA, and water transfer is that of Tardieu and Davies (1993), in which stomatal conductance depends on the concentration of ABA in the xylem sap and on the water potential at evaporative sites, supposed to be equal to Ψ_{bundle}. LER depends on xylem water potential with a linear relationship, consistent with that between nighttime LER and predawn leaf water potential (Reymond et al., 2003; Welcker et al., 2011). A minor effect of ABA on LER was added via a relationship between LER and the concentration of ABA in the xylem sap, as described by Tardieu et al. (2010). This was necessary to account for the effect of ABA in transgenic plants (Fig. 7; Parent et al., 2009).

The model outputs predicted large differences in time courses between the water potentials in the xylem and in mature cells of leaves. The latter closely matched water potentials measured with a pressure chamber (Fig. 9, A–C), and so did measured and simulated plant transpirations (data not shown). The simulated xylem water potential reacted very rapidly to a change in evaporative demand in the morning or to a soil rehydration. It recovered more rapidly than Ψ_{cell} in the afternoon, when the flux from mature cells to bundle sheaths reversed. The same pattern of recovery rates occurred in the rehydration experiment, in which Ψ_{cell} lagged behind Ψ_{xyl} until the capacitance of mature cells was filled. LER, which essentially depended on Ψ_{xyl}, closely matched experimental time courses in the three simulated experiments. Plants differing in ABA synthesis were adequately simulated (for the rehydration experiment, see Parent et al., 2009). Several hypotheses or adjustments were necessary for matching simulated and experimental data. (1) A change in plant hydraulic

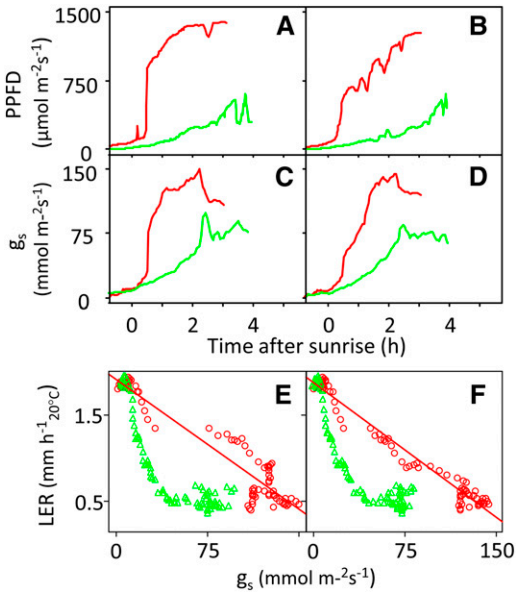

Figure 5. A to D, Time courses of PPFD (A and B) and stomatal conductance (g_s; C and D) of leaves receiving direct (red) or diffuse (green) sunlight during the morning (experiment 23 in Supplemental Table S1). E and F, Relationship between LER and stomatal conductance. r^2 = 0.91 and 0.97 for linear relations in E and F, respectively.

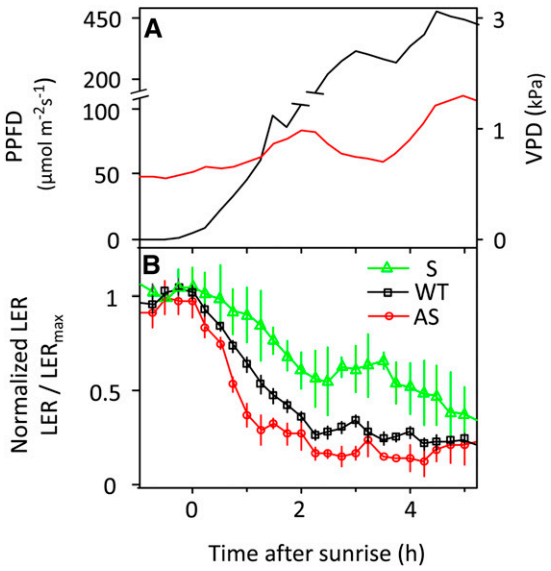

Figure 6. Time courses of environmental conditions and LER of well-watered plants of *NCED-VP14* AS, wild type (WT), and S plants (experiment 1 in Supplemental Table S1). A, Meristem-to-air VPD (red) and PPFD (black). B, LER divided by the mean LER in the same line during the night period. Error bars indicate confidence interval at $P < 0.05$.

conductance during the day was necessary for fitting the data, consistent with those observed experimentally. R_c between bundle sheaths and mature cells also had to vary during the day. We assumed in the model that these resistances changed with light, but the increase in conductance in the morning had to be quicker than the decline in the afternoon to fit the experimental data. (2) We could not simulate the 25-min lag time that elapsed between soil rehydration and the beginning of recovery of leaf water potential, so simulations began at the time when measured LER and Ψ_{xyl} began to increase. Overall, the model captured the main features of the experimental data, namely the synchrony between stomatal conductance and LER in the morning, the quicker changes in LER than in whole-plant transpiration, and the quicker changes in LER than in leaf water potential. This suggests that the observed data are compatible with a hydraulic model.

A Transcriptome Analysis Suggests Possible Contributions of Other Processes Involving the Synthesis of New Transcripts

A genome-wide transcriptome analysis was performed in the leaf growth zone, sampled 30 min before dawn (0 h) and 1.5 and 3 h after sunrise. Overall, the transcripts of 284 among 38,532 putative genes present on the chip varied significantly. Genes involved in light reactions (photosynthesis) were the major group exhibiting variations (60 putative genes) and were predominantly up-regulated in the morning (41 genes; Supplemental Fig. S5). Transient regulations (up/down or down/up) were dominated by genes involved in hormone biosynthesis or sensitivity and cell wall expansion. The group of genes involved in RNA splicing and degradation, RNA helicase and ribonucleases, and transport (membrane intrinsic proteins, ATP-binding cassette, cation and anion transporters) compose the major part of the cluster whose genes had transcript levels continuously declining. As expected, part of the circadian clock core oscillator genes promptly reacted after sunrise (Supplemental Fig. S6).

Six putative expansin genes, including expansins α4 and β2 directly linked to maize leaf growth (Muller et al., 2007), displayed a transient increase followed by a reduction in transcript abundance, while one expansin presented the opposite pattern (Supplemental Fig. S7A). Two genes encoding xyloglucan endotransglucosylase/hydrolase proteins showed a transient reduction (Supplemental Fig. S7B), and three putative genes of the glycosyl hydrolase family presented the opposite trend (data not shown). Three putative genes predicted to contribute to the cell wall structure (UDP-glucuronate 4-epimerase6 [Usadel et al., 2004], Man-1-P guanyltransferase [Lukowitz et al., 2001], and pectate lyase

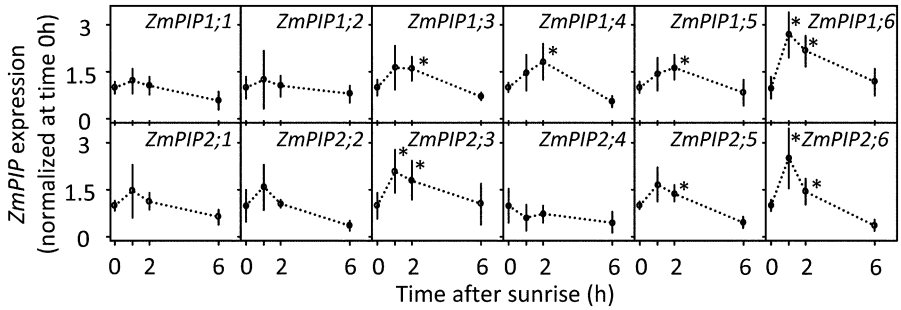

Figure 7. Expression levels (measured by quantitative reverse transcription-PCR) of 12 *ZmPIP* genes in roots during the morning. Samples were collected from plants grown in soil substrate (experiment 6 in Supplemental Table S1) during the morning (30 min before dawn [0 h] and 1, 2, and 6 h after sunrise). The geometric mean of the expression level of three control genes (*ACT1*, *EF1-α*, and *POLYUBIQUITIN*) was used to normalize the data. Each point represents a mean value (n = 3–5). Error bars indicate confidence intervals at the 0.95 risk level. Asterisks indicate significant variation ($P > 0.05$) of expression levels related to time 0 h in a Kruskal-Wallis test.

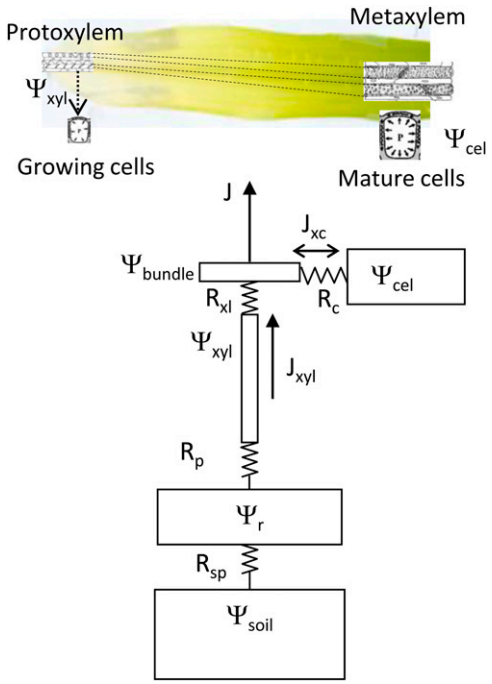

Figure 8. Schematic representation of the hydraulic model. Ψ_{soil}, Water potential of the soil surrounding roots during the night, close to the predawn water potential. Ψ_r, Water potential at the outer root surface, connected with Ψ_{soil} via a resistance, R_{sp}, that depends on soil hydraulic conductivity (a function of Ψ_{soil}) and root density. Ψ_{xyl}, Water potential in the leaf xylem at the leaf base (close to the elongating zone), connected to Ψ_r via a resistance, R_p, that changes with light intensity. Ψ_{bundle}, Water potential of bundle sheaths connected to Ψ_{xyl} with a resistance, R_{xl}. Ψ_{cell}, Water potential in cells of mature parts of the leaf, represented by a compartment that has a capacitance and is related to Ψ_{bundle} with a resistance, R_c, that changes with light intensity. Ψ_{cell} is equivalent to leaf water potential in Figures 2 to 4. J_{xyl}, Water flux in the xylem; J_{xc} water flux between bundle sheaths and mature cells; J transpiration flux, sum of J_{xyl} and J_{xc}. [See online article for color version of this figure.]

[Youssef et al., 2013]) had transcripts that continuously decreased during the morning (Supplemental Fig. S7C). ABA biosynthesis and ABA-responsive gene transcripts tended to increase after sunrise. In particular, transcripts of the *VP14* gene (Schwartz et al., 1997; Tan et al., 1997) displayed a transient increase and those of zeaxanthin epoxidase increased and stayed at high values (Supplemental Fig. S7D). ABA-responsive genes showed transcripts continuously increasing (two genes) or increasing followed by a decrease (six genes; Supplemental Fig. S7E). Tendencies were not straightforward for other hormones (Supplemental Fig. S7, F–H).

DISCUSSION

The Half-Time of LER Time Courses Is Compatible with a Hydraulic Control of Leaf Growth under Water Deficit

The time courses of the decline of LER during early morning and of its recovery after soil rehydration or in the evening had a common half-time of 20 to 30 min. These rapid responses could be expected for the effects of evaporative demand in view of published time courses involving fast changes in VPD in growth chambers (Ben Haj Salah and Tardieu, 1997; Munns et al., 2000) but not necessarily for the effect of water deficit, often considered as being longer term. They are compatible with hydraulic processes but also with posttranslational protein modifications such as phosphorylation/dephosphorylation (Novak et al., 2010; Bonhomme et al., 2012) or with the transfer of a plant hormone such as ABA over short distances from the apoplast to the symplast (Hartung et al., 2002). They are not necessarily compatible with mechanisms involving the synthesis of new transcripts and protein, the trafficking of the latter toward sites of action, and their effects on growth. This would potentially exclude the de novo synthesis of hormones, changes in cell wall composition, or changes in the rate of the cell cycle. In the latter case, changes in the timing of cell cycle transitions can occur over short times, but their consequences on growth are expected to occur slowly because it takes more than 1 d for a new cell to cross the elongating zone of maize leaves (Ben Haj Salah and Tardieu, 1997).

Time courses of LER were similar to those of stomatal conductance, thereby suggesting that changes in water transport contribute to the observed fast changes of LER. The fact that lines displaying different ABA biosynthesis rates differed in time courses (i.e. shorter half-time for lines producing less ABA) is compatible with this view, even though ABA affects many processes, including hydraulic conductivity (Parent et al., 2009), and cell wall properties (Curvers et al., 2010).

Posttranslational protein modifications may also make an appreciable contribution to rapid changes in LER upon soil rehydration. In an experiment involving a similar protocol of soil rehydration to that in Figure 4, with the same maize line, Bonhomme et al. (2012) showed that 40% of the phosphopeptides affected by water deficit displayed half-recovery of their phosphorylation status during the first 1 h of rehydration. Three and six phosphorylation sites recovered as early as 5 and 10 min after rewatering, respectively.

The change in transcript abundance in the transcriptome analysis did not suggest any other clear candidate than PIPs for rapid changes in LER. In particular, proteins involved in cell wall mechanical properties (Cosgrove, 2005) showed patterns a priori not consistent with a clear effect on growth, as did genes involved in hormone synthesis or sensitivity. In contrast, *PIP* transcripts in roots showed a consistent temporal pattern, with a rapid increase in transcript abundance 1 h after sunrise.

The Synchrony of LER with Stomatal Conductance, Not with Transpiration or Leaf Water Potential, Could Be a Consequence of the Hydraulic Architecture of Monocotyledon Leaves

Our findings suggest either an effect depending on the early stomatal aperture rather than on its consequences

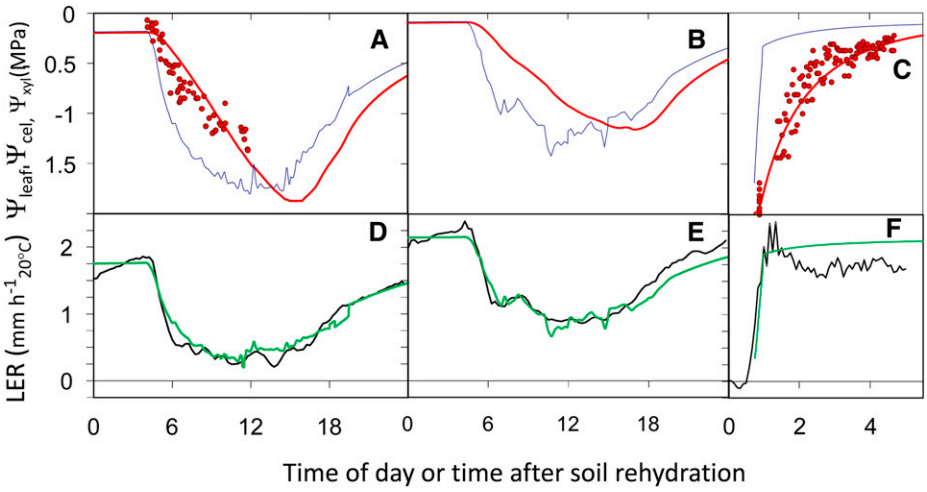

Figure 9. Outputs of the model presented in Figure 8, run with environmental conditions of 2 d with high (A and D; experiment 6) or low (B and E; experiment 9) evaporative demands or in the rehydration experiments (C and F; experiment 2–4). A to C, Red line, leaf water potential (Ψ_{leaf} [Ψ_{cell} in Fig. 8]); blue line, Ψ_{xyl}; red circles, Ψ_{leaf} measured experimentally. D to F, Green and black lines show simulated and observed LER, respectively.

on whole-plant transpiration rate, or a signaling mechanism collectively affecting both stomatal conductance and LER in the morning, for instance under the control of the circadian clock (Nozue et al., 2007). The latter view would require strong hypotheses to be compatible with the close synchrony of LER and stomatal conductance with sunrise regardless of time of day or with the results of experiments involving soil rehydration or lines differing in ABA synthesis. The model presented here is more parsimonious in hypotheses.

In monocotyledon leaves, the water status of the growing zone and of the xylem markedly differs from that of mature tissues (Martre et al., 1999). Indeed, mature tissues are located downstream of the growing zone, with a hydraulic connection that is not perfect because minor veins are still at a protoxylem stage (Martre et al., 2000). In addition, mature tissues have an appreciable capacitance, resulting in the relatively slow recovery of leaf water potential upon rehydration, while the xylem vessels have virtually no capacitance because they are rigid. The model developed on this base raises the possibility that early stomatal opening causes a severe decrease in the water potential in the xylem and/or in the elongating zone of the leaf, thereby affecting LER, whereas transpiration increases slowly because evaporative demand is still low at that time of day. In the same way, the rapid recovery of LER upon rehydration would be linked to the rapid increase of the water potential of the xylem and of the elongating zone, while that of mature tissues recovers more slowly because of a high capacitance and a partial hydraulic connection with elongating tissues. It is noteworthy that, in these transient conditions, the water potential of covered leaves did not follow LER better than the leaf water potential of uncovered leaves. It is often considered that the water potential of covered leaves is similar to xylem water potential because of the lack of flux inside the leaf (Simonneau and Habib, 1994). This is correct in the steady state but probably not in transient conditions, because the water potential measured with a pressure chamber is that of mature cells that present an appreciable capacitance.

The Increase in Plant Hydraulic Conductance in the Early Morning Limited the Decline of LER, Especially in Well-Watered Conditions

The plant hydraulic conductance increased during the morning, consistent with earlier reports (Lopez et al., 2003; Sakurai-Ishikawa et al., 2011; Hachez et al., 2012). This limited the decline in LER due to stomatal opening, consistent with the model that could not predict experimental data of LER without an appreciable increase in plant conductance. The more rapid decline of LER in plants underproducing ABA is consistent with a major contribution of hydraulic conductivity (Parent et al., 2009) and of a faster stomatal opening in the morning, with the opposite trends in plants overproducing ABA. In the same way, the more rapid decline of LER under moderate water deficit was probably linked to a lower contribution of plant hydraulic conductivity to the total conductance from soil to leaves, as predicted in the model. In a wet soil (−0.01 MPa), plant hydraulic conductance is lower than soil hydraulic conductance, thereby making the major contribution to limiting water movements. This is not the case at −0.15 MPa (Draye et al., 2010).

Changes in *PIP* transcript amounts during the morning were synchronous with those of plant hydraulic conductance. Diurnal change of gene and/or protein expression of most PIPs was previously reported in maize roots and mature parts of the leaf, but not in the leaf elongation zone (Lopez et al., 2003; Hachez et al., 2008, 2012). However, PIP phosphorylation, resulting in increased water channel activity, is also likely to occur in the early morning, as it is ubiquitous in the control of PIP activity (Maurel et al., 2008; Van Wilder et al., 2008). Furthermore, aquaporins in veins affect hydraulic conductivity in a light-dependent manner involving phosphorylation in Arabidopsis (*Arabidopsis thaliana*; Prado

et al., 2013). The rapid phosphorylation events discussed above may also affect the plant hydraulic conductivity upon soil rehydration, although the latter tends to decrease rather than increase during water deficit (Vandeleur et al., 2009).

It is not possible to fully disentangle here the different causes of changes in hydraulic conductivity during the early morning, such as a hydraulic trigger, a light signal, or circadian oscillations. Hydraulic signals generated by a fast increase in transpiration rate are associated with an increase in root hydraulic conductivity in rice (*Oryza sativa*; Sakurai-Ishikawa et al., 2011). Temperature and/or light signals affect the hydraulic conductance of walnut (*Juglans regia*) leaves as well as the transcript abundance of the aquaporins *JrPIP2;1* and *JrPIP2;2* (Cochard et al., 2007). Circadian oscillations affect aquaporin genes and plant hydraulic conductivity in Arabidopsis (Takase et al., 2011). We have recently shown that circadian oscillations of LER, hydraulic conductance, and *PIP* transcripts (observed in continuous light) are entrained in maize by oscillations of leaf water status during previous days (C.F. Caldeira, L. Jeanguenin, F. Chaumont, and F. Tardieu, unpublished data). Our model required a faster response of hydraulic conductance to light in the morning than in the afternoon, consistent with a circadian effect on hydraulic conductance in addition to an effect of light or of transpiration rate.

The Hydraulic Trigger of Changes in LER Does Not Rule out Nonhydraulic Mechanisms in the Elongating Zone

Mechanisms other than hydraulics participate in the changes in LER with water deficit. The concentration of ABA increases in plants subjected to water deficit and may contribute to a limitation of leaf growth, with in some species a contribution of the apoplastic pH and ethylene (Sobeih et al., 2004; Wilkinson and Davies, 2008). It has been argued recently that the direct effect of ABA might be less than once believed, while its effects on plant hydraulics via stomatal conductance and tissue hydraulic conductivity may be prominent (Tardieu et al., 2010). The same authors argued that the apparently systemic effect observed in split-root experiments (Davies and Zhang, 1991) may have a hydraulic interpretation. In addition, changes in evaporative demand are usually not accompanied by an increase of ABA concentration in the xylem sap (Tardieu and Davies, 1993), so ABA alone cannot account for the decrease in LER during the day.

Our model suggests that a hydraulic process may account for the rapid changes in LER upon changes in evaporative demand or soil water content. While the synchrony of LER and xylem water potential is a feature of the model, the mode of action of this synchrony is not explicit in the model. It is compatible with a change in the turgor of growing cells (Ehlert et al., 2009) or in the gradient of water potential between growing cells and the xylem (Tang and Boyer, 2002, 2008). It might also involve rapid changes in cell wall properties triggered by a hydraulic signal. Indeed, the rapid phosphorylation events observed by Bonhomme et al. (2012) may trigger rapid changes in cell wall mechanical properties. They also could affect the activity of PIP proteins (Maurel et al., 2008; Van Wilder et al., 2008).

CONCLUSION

The hydraulic processes presented here probably have a negligible effect in growth chamber studies with stable environmental conditions and in controlled or natural conditions in which water deficit is so severe that water fluxes are strongly limited by stomatal conductance. However, if one considers that stability of evaporative demand and soil water status is, in most conditions, an exception rather than a rule (with rapid changes in evaporative demand due to clouds and of soil water availability from small rains or dew), the hydraulic mechanisms presented here may appreciably contribute to changes in final leaf area with environmental conditions and to the genetic variability of these changes. This is supported by genetic analyses showing a community of quantitative trait loci between (1) the sensitivities of LER to soil water deficit and to evaporative demand (Welcker et al., 2011), (2) the time course of the morning decline of LER and the overall sensitivity of LER to evaporative demand calculated over 1 week (Sadok et al., 2007), and (3) the genetic control of LER and of final leaf area (Dignat et al., 2013).

MATERIALS AND METHODS

Genetic Material

The standard maize (*Zea mays*) inbred line B73 and a series of transformed maize lines were analyzed. Lines affected in the *NCED/VP14* gene were constructed as described by Parent et al. (2009). AS lines displayed low ABA concentration in the xylem sap, high stomatal conductance and transpiration rate, low root PIP aquaporin mRNA levels and proteins amounts, and consequently low root hydraulic conductivity. The S line presented the opposite traits when compared with the wild type (null transformed) plants (Parent et al., 2009).

Plant Growth Conditions in the Greenhouse

Twenty-three experiments (Supplemental Table S1), 22 of them with line B73, were carried out in the Phenodyn platform (http://bioweb.supagro.inra.fr/phenodyn/; Sadok et al., 2007). Plants were grown in polyvinyl chloride columns (0.23-m diameter and 0.4-m height) containing a 40:60 (v/v) mixture of filtered loamy soil (particle diameter ranging from 0.1–4 mm) and organic compost. Air temperature and relative humidity were measured at the plant level every 30 s with nine sensors (HMP35A; Vaisala Oy). The temperature of the meristematic zone was measured with fine copper-constantan thermocouples (0.2-mm diameter) inserted between the sheaths of leaves 2 and 3 of six plants per experiment. PPFD was measured every 30 s using nine sensors (LI-190SB from Li-Cor and SOLEMS 01/012/012). Meristem-to-air vapor pressure difference was estimated at each time step as the difference in water vapor pressure between saturation at meristem temperature and the current vapor pressure in the air. All climatic data were averaged and stored every 15 min in a data logger (Campbell Scientific LTD-CR10X Wiring Panel).

Soil water content was measured by weighing columns automatically every 15 min. Differences in weight were attributed to changes in soil water content,

after correction for the increase in mean plant biomass as a function of phenological stage and for the effect of displacement transducers. A water-release curve of the soil was obtained by measuring the soil water potential of soil samples with different water contents, in the range 0.4 to 0.2 g g^{-1} (WP4-T Dewpoint Meters; Decagon Devices), allowing calculation of the mean soil water potential in each soil column every 15 min. In the experiments performed in well-watered conditions, the soil substrate was maintained at retention capacity by daily watering with a modified one-tenth-strength Hoagland solution. The same solution was used in experiments realized under mild water deficit (−0.15 and −0.6 MPa). All climatic data were averaged and stored every 15 min in a data logger (Campbell Scientific LTD-CR10X Wiring Panel). Supplemental light was used during the winter to keep the photoperiod at 12 h of light and 12 h of dark and photosynthetic photon flux density at more than 400 μmol m^{-2} s^{-1}.

Plant Growth Conditions in Hydroponics

Maize seeds were germinated in petri dishes at 20°C in the dark and saturated air. After 4 d, seedlings were placed in tubes with mineral fibers and transferred to the greenhouse with their roots bathing in a continuously aerated solution. The composition of solution was as follows: 0.25 mM $CaSO_4$, 0.8 mM KNO_3, 0.6 mM KH_2PO_4, 0.2 mM $MgSO_4$-$7H_2O$, 0.4 mM NH_4NO_3, 2×10^{-3} mM $MnSO_4$, 0.4×10^{-3} mM $ZnSO_4$, 0.4×10^{-3} mM $CuSO_4$, 0.2×10^{-3} mM Na_2MoO_4-$2H_2O$, 1.6×10^{-2} mM H_3Bo_3, 0.04 mM Fe-EDDHA, and 2.5 mM MES, pH 5.5 to 6. The hydroponic solution was renewed every third to fourth day, and the pH was controlled every day. The water deficit treatment were applied by replacing the standard nutrient solution by a nutrient solution containing mannitol (Sigma-Aldrich), corresponding to a water potential of −0.15 MPa, checked with a vapor pressure osmometer (Vapro 5520; Wescor). Mannitol treatment was applied at the end of day preceding the measurements. Environmental data were measured and stored as above.

Plant Measurements

LER was measured with rotational displacement transducers (601-1045 Full 360° Smart Position Sensor; Spectrol Electronics). A pulley was attached to the sensor, which carried a copper thread clipped to the leaf tip and to a 20-g counterweight. LER was averaged and stored every 3 min in most experiments and every 5 or 15 min in some of them, after correction of the effect of temperature on thread length. In all experiments, measurements began when the tip of the sixth leaf appeared above the whorl and lasted until the appearance of leaf 8. This period corresponds to a plateau during which LER is stable (Sadok et al., 2007). LER was expressed in thermal time, via equivalent days at 20°C (Parent et al., 2010), to account for the direct effect of temperature fluctuations.

Transpiration rate was calculated from the weight loss of each column divided by the plant leaf area. Direct evaporation from the soil was estimated by measuring the weight loss of columns carrying plastic plants, whose upper layer was watered in such a way that its water content was similar to that of the studied columns. Transpiration rate was averaged and stored every 15 min. Leaf area was calculated from the length and width of each leaf of 60 plants every second day. A logistic model was fitted to the time course of the area of each leaf. Plant leaf area was obtained every day by determining the area of all leaves.

The time courses of climatic variables, leaf elongation, and transpiration rate obtained in the 23 experiments were classified into a limited scenario type. Clusters of daily time courses were obtained in three steps using the R language (R Development Core Team, 2013). Raw data were classified by (1) the nature of day/night transitions and photoperiod of each experiment: fast day/night transitions occurred in the autumn/winter experiment because additional light was supplied, while spring/summer experiments had slower transitions in the absence of additional light; (2) soil water availability, which differed between experiments, was classified into well watered (−0.1 to 0 MPa), mild water deficit (−0.2 to −0.1 MPa), and water deficit (−0.6 to −0.4 MPa); (3) evaporative demand, which essentially depends on PPFD and VPD, was classified in sunny (PPFD > 1,000 μmol m^{-2} s^{-1} and VPD > 1.5 kPa at midday), cloudy (PPFD < 300 μmol m^{-2} s^{-1} and VPD < 1.5 kPa), plus intermediate classes. Twenty-four-hour time courses corresponding to one plant were averaged and considered as one repetition in further analyses to obtain the mean values and confidence intervals of time courses in a given scenario. The half-times of the variations of LER, leaf water potential, and transpiration rate during the morning and during recovery were calculated after interpolation using the R function *spline* (R Development Core Team, 2013). The maximum and minimum values were entered into the *spline* function. The half-time was calculated as the time at which the function value was the mean of minimum and maximum values.

Leaf water potential was measured in nonexpanding leaves with a pressure chamber (Soil Moisture Equipment). The water potential of covered leaves was measured after covering the considered leaf first with a transparent plastic bag to prevent transpiration and then wrapped with aluminum foil to avoid excessive increase in temperature. Leaves were prepared during the evening of the day preceding the measurements.

Stomatal conductance was measured every minute with a gas analyzer (CIRAS-2; PP Systems) in experiment 23. Two gas analyzers were used simultaneously: one was placed on a leaf part facing the first sunbeams and the other one on the opposite side of the plant receiving diffuse light. Stomatal conductance was also measured in experiment 5 (hydroponics) on leaves receiving direct sunlight using a diffusion porometer (AP4; Delta-T Devices) calibrated every 30 min.

Whole-plant hydraulic conductance was calculated from the water loss per plant, divided by the difference between soil and leaf water potentials. Transpiration and soil water potential were calculated every 15 min as presented above. Mean values of leaf water potential were obtained from the measures performed during the last 5 min corresponding to each time step of 15 min. Root hydraulic conductivity was measured in plants hydroponically grown in the greenhouse. The free exudation rate of the excised root system was measured by collecting exuded sap with tubes filled with cotton fibers and weighing it. The osmotic potentials of the sap and of the nutrient solution were measured with a vapor pressure osmometer (Vapro 5520; Wescor). The root hydraulic conductivity on an osmotic gradient (Lp_{os}) was calculated as follows:

$$Lp_{os} = J * (\pi_{sap} - \pi_{sol})^{-1} * A^{-1} \quad (1)$$

where J is the water flux through the root system (mg m^{-2} s^{-1}), π_{sap} and π_{sol} (MPa) are the osmotic potentials of the sampled sap and of the nutrient solution, respectively, and A is the area of the root system (m^2).

Rewetting Experiments in Controlled Conditions

Plants (line B73) were grown in the greenhouse with mild water deficit (soil water potential of −0.4 MPa). At the seven-visible-leaf stage, they were transferred at noon to a growth chamber with a high evaporative demand (VPD = 2.8 kPa, 28°C, PPFD = 600 μmol m^{-2} s^{-1}). They were left to transpire under these conditions for 6 h, during which leaf water potential was measured with a pressure chamber and LER of the sixth leaf was monitored every 5 min with rotational displacement transducers as described above. At time 0, plants were rewatered to retention capacity and placed in dark conditions at VPD of 0.8 kPa, which virtually stopped transpiration. LER and leaf water potential were measured every 3 min for the 5 h following rehydration. This experiment was repeated three times.

Quantitative Reverse Transcription-PCR

Quantitative reverse transcription-PCR was carried out with total RNA extracted from elongating tissues of leaves (6 cm behind the leaf insertion points of leaves 7, 8, and 9) and the 5 cm behind root tips. Tissues were sampled 30 min before sunrise (0 h) and 1, 2, and 6 h after it in both roots and the elongating zone of the leaf. Tissues were flash frozen in liquid nitrogen less than 30 s after sampling. Leaf and root tissues were ground with a Mixer Mill 400 MM (Retsch), and total RNA was extracted using the Spectrum Plant Total RNA Kit (Sigma). DNase digestion was performed on column during RNA extraction according to the manufacturer's recommendations. Complementary DNA (cDNA) synthesis and real-time PCR were performed as described earlier (Hachez et al., 2006). Data were analyzed by the $2^{-\Delta\Delta Ct}$ method (Pfaffl, 2001) and normalized using three reference genes, *ACTIN1* (accession no. gi: 450292), *ELONGATION FACTOR1-α* (gi: 2282583), and *POLYUBIQUITIN* (gi: 248338). This approach minimizes normalization errors resulting from small variations in the expression of individual reference genes (Vandesompele et al., 2002). Background noise level was determined by the cycle threshold number of a negative control without template. Signals were considered specific when the cycle threshold value was lower (higher expression) than the respective negative control without template value.

Microarray Processing and Analysis

The oligonucleotide microarray Maïs 45K BGA (Roche NimbleGen) displays a set of 45,000 probes designed using pseudomolecules and gene models (FilterGeneSet) provided by the Maize Genome Sequencing Project (www.maizesequence.org; version 4a53), allowing to each probe a corresponding maize gene identifier. One to three probes were used to represent a gene. A total of 2,563 random probes were used for technical and internal hybridization controls. The growing zone of leaves was collected 30 min before sunrise and 1.5 and 3 h after it in the experiment exhibited in Figure 2A. Three samples were collected at each sampling time and flash frozen less than 30 s after sampling. Total RNA was isolated from the tissues with the RNeasy Plant Mini Kit (Qiagen) following the manufacturer's protocol. After controlling the RNA integrity by capillary electrophoresis (Bioanalyzer; Agilent), cDNA was synthesized using the SuperScript Double-Stranded cDNA Synthesis Kit (Invitrogen/Fisher; Bioblock W34277). The cDNAs were then purified by a phenol/chloroform step and further labeled with Cy3 fluorescent dye (One-Color DNA Labeling kit; Roche NimbleGen). After overnight hybridization (16 h at 42°C), the microarray slides were washed and scanned with an MS200 Roche NimbleGen scanner. The laser power settings were optimized to the Autogain mode, which determine the optimal range of acquisition for each scan (laser power was fixed at 100%). The microarrays were scanned three times, and the images were inspected visually for image artifacts. Intensities were extracted, filtered, and normalized with the NimbleScan software. Raw hybridization intensities were normalized across all arrays with RMA Express, in which the quantile normalization method was employed (Bolstad et al., 2003).

Data were imported into R (R Development Core Team, 2013). The $\log_2$ of the transcript abundance was calculated for each probe. Change with time of the transcript abundance corresponding to a given probe was considered as significant if (1) the q value (P value after false discovery rate correction) was lower than 0.05 in Student's t test and (2) it differed by a factor larger than 1.5 between times of sampling. Patterns were calculated by considering the dawn value as the reference; that is, values shown in Supplemental Figures S6 and S7 are $\log_2(t_0/t_n)$, where t_0 and t_n are the values at dawn and at time n. Functional annotation was enriched with homologous genes of other species identified by BLASTp against plant protein sequences from UniProt (http://www.uniprot.org/) and rice (*Oryza sativa*) protein sequences (Michigan State University Rice Genome Annotation Project release 6.0). The classes of genes presented in Supplemental Figure S5 were prepared following the ontologies proposed in MapMan (http://gabi.rzpd.de/projects/MapMan) with the maize genome release Zm_B73_5b_FGS_cds_2012 (http://mapman.gabipd.org/web/guest/mapmanstore).

Model of Water Transfer

The model is derived from that of Tardieu and Davies (1993), run at a time step of 1 min. Water flows between compartments following Ψ_{soil} to Ψ_r, Ψ_{xyl}, and Ψ_{bundle}. Ψ_{soil} is an equivalent of that proposed by Couvreur et al. (2012) to represent the water potential of the soil surrounding roots during the night, close to predawn water potential. Ψ_r represents the water potential at the outer root surface. The resistance R_{sp} (MPa s plant mg^{-1}) between both compartments was calculated as in Gardner (1960)

$$\ln\left(d^2/r^2\right)/4\pi\, k(\theta) \tag{2}$$

where d and r are the mean distance between neighboring roots and root radius, respectively, and $k(\theta)$ is the soil hydraulic conductivity as a function of soil water content, as calculated by Van Genuchten (1980). Ψ_{xyl} stands for the water potential in the leaf xylem near the leaf insertion point, close to the elongating zone (Fig. 8), depending on a resistance, R_p (MPa s plant mg^{-1}), that summarizes the resistances in root tissues and in the plant xylem. It was assumed to depend linearly on PPFD. Because the model could only fit experimental results if R_p decreased more slowly in the afternoon than it increased in the morning, the dependence of R_p on PPFD was calculated at step i in the morning with parameters calculated on data presented in Figure 2 and at step i-3 h in the afternoon with the same parameters. The Ψ_{bundle} is assumed to be connected to Ψ_{xyl} with a resistance, R_{xl} (MPa s plant mg^{-1}), that was very small in the vector of parameters finally considered in the model, so it was not necessary to assume a dependence on PPFD. Ψ_{bundle} is the water potential assumed to affect stomatal conductance in Equation 7. Ψ_{cell} stands for leaf water potential in cells of mature parts of the leaf, represented by a compartment that has a capacitance and is related to Ψ_{bundle} with a resistance, R_c (MPa s plant mg^{-1}). The capacitance was calculated using the pressure volume curve of Tardieu et al. (1992) and Parent et al. (2009). It was fitted on the formalism of Van Genuchten (1980). R_c was fitted on the results of the rehydration experiment (Fig. 4). The flux J_{xc} (mg plant^{-1} s^{-1}) between this compartment and Ψ_{bundle} was calculated following the gradient of water potential between both compartments with a resistance, R_c, that depended on PPFD in the same way as R_p. Therefore, we solved the differential equation for calculating the cell water potential Ψ_{cel} and J_{xc}.

$$J_{xc} = dV_{cell}/dt = (\Psi_{bundle} - \Psi_{cel})/R_c \tag{3}$$

$$V_{cell} = V_{res} + (V_{sat} - V_{res}) * (1/\{1 + [\alpha\star(-\Psi_{cel})]^n\})^{(1-1/n)} \tag{4}$$

where V_{sat} (mm^3) is the leaf volume at saturation, and V_{res} is the residual water volume −0.3 MPa, and α and n are the parameters of a Van Genuchten equation fitted on the pressure volume curve. J_{xc} was calculated as the difference in V_{cell} between two different times for the optimization process of resolution of the differential equation. At each time i, the flux through roots and xylem is the sum of the transpiration flux J and of J_{xc}.

The model calculates stomatal conductance, the concentration of ABA in the xylem sap ($[ABA]_{xyl}$), water flux, root, and the water potentials in transpiration sites from soil water potential, light intensity, and air VPD. Stomatal conductance is calculated as described by Tardieu and Davies (1993).

$$g_s = g_{smin} + \alpha\exp\left[\beta[ABA]_{xyl}\exp(\delta\Psi_{bundle})\right] \tag{5}$$

where g_{smin} is the minimum stomatal conductance resulting from cuticular conductance and conductance through closed stomata. α, β, and δ are the parameters proposed by Tardieu and Davies (1993). The transpiration flux J is calculated with the Penman Monteith equation but taking into account plant leaf area in order to express transpiration per plant. $[ABA]_{xyl}$ is calculated as described by Tardieu and Davies (1993).

$$[ABA]_{xyl} = -a\Psi_r/(J + b) \tag{6}$$

The model first solves every 1 min the five equations with five unknowns, namely the Penman Monteith equation, Equations 1, 6, and 7, and the equation relating J to the difference in potential between Ψ_{bundle} and Ψ_r divided by the resistance R_p. It then solves Equations 3 and 4 every 1 min. Finally, LER is calculated as a maximum rate, genotype dependent, which is affected by ln $[ABA]_{xyl}$ as described by Tardieu et al. (2010; with a minor effect, a_r_aba) and by Ψ_{xyl} in a linear fashion (parameters a_ler and c_ler), as described by Welcker et al. (2011).

$$LER = a\_ler + \min\left(0, -a\_r\_aba * \ln[ABA]_{xyl} * \left(1 + c\_ler * \Psi_{xyl}\right)\right) \tag{7}$$

The model was implemented in the R language.

Supplemental Data

The following materials are available in the online version of this article.

Supplemental Figure S1. Daily time courses of environmental conditions, J and LER, and the relationship between LER and J in six groups of experiments.

Supplemental Figure S2. Daily time courses of environmental conditions, J and LER, and the relationship between LER and J in five groups of experiments.

Supplemental Figure S3. Half-times of reductions in LER and of increase in J during the morning in 13 experiments.

Supplemental Figure S4. Expression levels of 12 *ZmPIP* genes in the leaf growth zone during the morning.

Supplemental Figure S5. Overview of the genome-wide transcriptome analysis performed in the growing zone of leaves sampled 30 min before dawn, and 1 h 30 min and 3 h after sunrise.

Supplemental Figure S6. Time courses of the ratio of expression levels of the core oscillator genes in the leaf growing zone and roots of plants grown in soil.

Supplemental Figure S7. Patterns of ratio of expression level of genes associated with cell wall expansion, phytohormone biosynthesis, and phythormone response.

Supplemental Table S1. Environmental conditions and lines used in the 23 experiments. Mean half times of the time courses of LER and J during early morning.

Received September 12, 2013; accepted December 22, 2013; published January 13, 2014.

LITERATURE CITED

Bacon MA, Thompson DS, Davies WJ (1997) Can cell wall peroxidase activity explain the leaf growth response of Lolium temulentum L. during drought? J Exp Bot **48:** 2075–2085

Baerenfaller K, Massonnet C, Walsh S, Baginsky S, Bühlmann P, Hennig L, Hirsch-Hoffmann M, Howell KA, Kahlau S, Radziejwoski A, et al (2012) Systems-based analysis of Arabidopsis leaf growth reveals adaptation to water deficit. Mol Syst Biol **8:** 606

Ben Haj Salah H, Tardieu F (1997) Control of leaf expansion rate of droughted maize plants under fluctuating evaporative demand (a superposition of hydraulic and chemical messages?). Plant Physiol **114:** 893–900

Bolstad BM, Irizarry RA, Astrand M, Speed TP (2003) A comparison of normalization methods for high density oligonucleotide array data based on variance and bias. Bioinformatics **19:** 185–193

Bonhomme L, Valot B, Tardieu F, Zivy M (2012) Phosphoproteome dynamics upon changes in plant water status reveal early events associated with rapid growth adjustment in maize leaves. Mol Cell Proteomics **11:** 957–972

Bray EA (1997) Plant responses to water deficit. Trends Plant Sci **2:** 48–54

Chazen O, Neumann PM (1994) Hydraulic signals from the roots and rapid cell-wall hardening in growing maize (*Zea mays* L.) leaves are primary responses to polyethylene glycol-induced water deficits. Plant Physiol **104:** 1385–1392

Cochard H, Venisse JS, Barigah TS, Brunel N, Herbette S, Guilliot A, Tyree MT, Sakr S (2007) Putative role of aquaporins in variable hydraulic conductance of leaves in response to light. Plant Physiol **143:** 122–133

Cosgrove DJ (2005) Growth of the plant cell wall. Nat Rev Mol Cell Biol **6:** 850–861

Couvreur V, Vanderborght J, Javaux M (2012) A simple three-dimensional macroscopic root water uptake model based on the hydraulic architecture approach. Hydrol Earth Syst Sci **16:** 2957–2971

Curvers K, Seifi H, Mouille G, de Rycke R, Asselbergh B, Van Hecke A, Vanderschaeghe D, Höfte H, Callewaert N, Van Breusegem F, et al (2010) Abscisic acid deficiency causes changes in cuticle permeability and pectin composition that influence tomato resistance to *Botrytis cinerea*. Plant Physiol **154:** 847–860

Davies WJ, Zhang JH (1991) Root signals and the regulation of growth and development of plants in drying soil. Annu Rev Plant Physiol Plant Mol Biol **42:** 55–76

Dignat G, Welcker C, Sawkins M, Ribaut JM, Tardieu F (2013) The growths of leaves, shoots, roots and reproductive organs partly share their genetic control in maize plants. Plant Cell Environ **36:** 1105–1119

Draye X, Kim Y, Lobet G, Javaux M (2010) Model-assisted integration of physiological and environmental constraints affecting the dynamic and spatial patterns of root water uptake from soils. J Exp Bot **61:** 2145–2155

Ehlert C, Maurel C, Tardieu F, Simonneau T (2009) Aquaporin-mediated reduction in maize root hydraulic conductivity impacts cell turgor and leaf elongation even without changing transpiration. Plant Physiol **150:** 1093–1104

Gardner WR (1960) Dynamic aspects of water availability to plants Soil Science **89:** 63–73

Granier C, Aguirrezabal L, Chenu K, Cookson SJ, Dauzat M, Hamard P, Thioux JJ, Rolland G, Bouchier-Combaud S, Lebaudy A, et al (2006) PHENOPSIS, an automated platform for reproducible phenotyping of plant responses to soil water deficit in Arabidopsis thaliana permitted the identification of an accession with low sensitivity to soil water deficit. New Phytol **169:** 623–635

Granier C, Inzé D, Tardieu F (2000) Spatial distribution of cell division rate can be deduced from that of p34(cdc2) kinase activity in maize leaves grown at contrasting temperatures and soil water conditions. Plant Physiol **124:** 1393–1402

Granier C, Tardieu F (1998) Spatial and temporal analyses of expansion and cell cycle in sunflower leaves: a common pattern of development for all zones of a leaf and different leaves of a plant. Plant Physiol **116:** 991–1001

Hachez C, Heinen RB, Draye X, Chaumont F (2008) The expression pattern of plasma membrane aquaporins in maize leaf highlights their role in hydraulic regulation. Plant Mol Biol **68:** 337–353

Hachez C, Moshelion M, Zelazny E, Cavez D, Chaumont F (2006) Localization and quantification of plasma membrane aquaporin expression in maize primary root: a clue to understanding their role as cellular plumbers. Plant Mol Biol **62:** 305–323

Hachez C, Veselov D, Ye Q, Reinhardt H, Knipfer T, Fricke W, Chaumont F (2012) Short-term control of maize cell and root water permeability through plasma membrane aquaporin isoforms. Plant Cell Environ **35:** 185–198

Hartung W, Sauter A, Hose E (2002) Abscisic acid in the xylem: where does it come from, where does it go to? J Exp Bot **53:** 27–32

Hsiao TC, Acevedo E, Henderson DW (1970) Maize leaf elongation: continuous measurements and close dependence on plant water status. Science **168:** 590–591

Kim BJ, Tersoff J, Kodambaka S, Reuter MC, Stach EA, Ross FM (2008) Kinetics of individual nucleation events observed in nanoscale vapor-liquid-solid growth. Science **322:** 1070–1073

Knowles TPJ, Waudby CA, Devlin GL, Cohen SIA, Aguzzi A, Vendruscolo M, Terentjev EM, Welland ME, Dobson CM (2009) An analytical solution to the kinetics of breakable filament assembly. Science **326:** 1533–1537

Lopez F, Bousser A, Sissoëff I, Gaspar M, Lachaise B, Hoarau J, Mahé A (2003) Diurnal regulation of water transport and aquaporin gene expression in maize roots: contribution of PIP2 proteins. Plant Cell Physiol **44:** 1384–1395

Lukowitz W, Nickle TC, Meinke DW, Last RL, Conklin PL, Somerville CR (2001) Arabidopsis cyt1 mutants are deficient in a mannose-1-phosphate guanylyltransferase and point to a requirement of N-linked glycosylation for cellulose biosynthesis. Proc Natl Acad Sci USA **98:** 2262–2267

Martre P, Bogeat-Triboulot MB, Durand JL (1999) Measurement of a growth-induced water potential gradient in tall fescue leaves. New Phytol **142:** 435–439

Martre P, Durand JL, Cochard H (2000) Changes in axial hydraulic conductivity along elongating leaf blades in relation to xylem maturation in tall fescue. New Phytol **146:** 235–247

Maurel C, Verdoucq L, Luu DT, Santoni V (2008) Plant aquaporins: membrane channels with multiple integrated functions. Annu Rev Plant Biol **59:** 595–624

Muller B, Bourdais G, Reidy B, Bencivenni C, Massonneau A, Condamine P, Rolland G, Conéjéro G, Rogowsky P, Tardieu F (2007) Association of specific expansins with growth in maize leaves is maintained under environmental, genetic, and developmental sources of variation. Plant Physiol **143:** 278–290

Munns R, Passioura JB, Guo J, Chazen O, Cramer GR (2000) Water relations and leaf expansion: importance of time scale. J Exp Bot **51:** 1495–1504

Novak B, Kapuy O, Domingo-Sananes MR, Tyson JJ (2010) Regulated protein kinases and phosphatases in cell cycle decisions. Curr Opin Cell Biol **22:** 801–808

Nozue K, Covington MF, Duek PD, Lorrain S, Fankhauser C, Harmer SL, Maloof JN (2007) Rhythmic growth explained by coincidence between internal and external cues. Nature **448:** 358–361

Parent B, Hachez C, Redondo E, Simonneau T, Chaumont F, Tardieu F (2009) Drought and abscisic acid effects on aquaporin content translate into changes in hydraulic conductivity and leaf growth rate: a trans-scale approach. Plant Physiol **149:** 2000–2012

Parent B, Turc O, Gibon Y, Stitt M, Tardieu F (2010) Modelling temperature-compensated physiological rates, based on the co-ordination of responses to temperature of developmental processes. J Exp Bot **61:**2057–2069

Pfaffl MW (2001) A new mathematical model for relative quantification in real-time RT-PCR. Nucleic Acids Res **29:** e45

Prado K, Boursiac Y, Tournaire-Roux C, Monneuse JM, Postaire O, Da Ines O, Schäffner AR, Hem S, Santoni V, Maurel C (2013) Regulation of *Arabidopsis* leaf hydraulics involves light-dependent phosphorylation of aquaporins in veins. Plant Cell **25:** 1029–1039

R Development Core Team (2013) R: A Language and Environment for Statistical Computing. R Foundation for Statistical Computing, Vienna

Reymond M, Muller B, Leonardi A, Charcosset A, Tardieu F (2003) Combining quantitative trait loci analysis and an ecophysiological model to analyse the genetic variability of the responses of leaf growth to temperature and water deficit. Plant Physiol **131:** 664–675

Sadok W, Naudin P, Boussuge B, Muller B, Welcker C, Tardieu F (2007) Leaf growth rate per unit thermal time follows QTL-dependent daily patterns in hundreds of maize lines under naturally fluctuating conditions. Plant Cell Environ **30:** 135–146

Sakurai-Ishikawa J, Murai-Hatano M, Hayashi H, Ahamed A, Fukushi K, Matsumoto T, Kitagawa Y (2011) Transpiration from shoots triggers diurnal changes in root aquaporin expression. Plant Cell Environ **34:** 1150–1163

Schnyder H, Nelson CJ (1988) Diurnal growth of tall fescue leaf blades. I. Spatial distribution of growth, deposition of water, and assimilate import in the elongation zone. Plant Physiol **86:** 1070–1076

Schwartz SH, Tan BC, Gage DA, Zeevaart JAD, McCarty DR (1997) Specific oxidative cleavage of carotenoids by VP14 of maize. Science **276:** 1872–1874

Schweizer FE, Dresbach T, DeBello WM, O'Connor V, Augustine GJ, Betz H (1998) Regulation of neurotransmitter release kinetics by NSF. Science **279:** 1203–1206

Simonneau T, Habib R (1994) Water uptake regulation in peach trees with split-root systems. Plant Cell Environ **17:** 379–388

Sobeih WY, Dodd IC, Bacon MA, Grierson D, Davies WJ (2004) Long-distance signals regulating stomatal conductance and leaf growth in tomato (Lycopersicon esculentum) plants subjected to partial root-zone drying. J Exp Bot **55:** 2353–2363

Takase T, Ishikawa H, Murakami H, Kikuchi J, Sato-Nara K, Suzuki H (2011) The circadian clock modulates water dynamics and aquaporin expression in Arabidopsis roots. Plant Cell Physiol **52:** 373–383

Tan BC, Schwartz SH, Zeevaart JAD, McCarty DR (1997) Genetic control of abscisic acid biosynthesis in maize. Proc Natl Acad Sci USA **94:** 12235–12240

Tang AC, Boyer JS (2002) Growth-induced water potentials and the growth of maize leaves. J Exp Bot **53:** 489–503

Tang AC, Boyer JS (2008) Xylem tension affects growth-induced water potential and daily elongation of maize leaves. J Exp Bot **59:** 753–764

Tardieu F, Davies WJ (1992) Stomatal response to abscisic acid is a function of current plant water status. Plant Physiol **98:** 540–545

Tardieu F, Davies WJ (1993) Integration of hydraulic and chemical signalling in the control of stomatal conductance and water status of droughted plants. Plant Cell Environ **16:** 341–349

Tardieu F, Parent B, Simonneau T (2010) Control of leaf growth by abscisic acid: hydraulic or non-hydraulic processes? Plant Cell Environ **33:** 636–647

Tardieu F, Zhang J, Katerji N, Bethenod O, Palmer S, Davies WJ (1992) Xylem ABA controls the stomatal conductance of field-grown maize subjected to soil compaction or soil drying. Plant Cell Environ **15:** 193–197

Usadel B, Schlüter U, Mølhøj M, Gipmans M, Verma R, Kossmann J, Reiter WD, Pauly M (2004) Identification and characterization of a UDP-D-glucuronate 4-epimerase in Arabidopsis. FEBS Lett **569:** 327–331

Vandeleur RK, Mayo G, Shelden MC, Gilliham M, Kaiser BN, Tyerman SD (2009) The role of plasma membrane intrinsic protein aquaporins in water transport through roots: diurnal and drought stress responses reveal different strategies between isohydric and anisohydric cultivars of grapevine. Plant Physiol **149:** 445–460

Vandesompele J, De Preter K, Pattyn F, Poppe B, Van Roy N, De Paepe A, Speleman F (2002) Accurate normalization of real-time quantitative RT-PCR data by geometric averaging of multiple internal control genes. Genome Biol **3:** RESEARCH0034

Van Genuchten MT (1980) A closed-form equation for predicting the hydraulic conductivity of unsaturated soils. Soil Sci Soc Am J **4:** 892–898

Van Wilder V, Miecielica U, Degand H, Derua R, Waelkens E, Chaumont F (2008) Maize plasma membrane aquaporins belonging to the PIP1 and PIP2 subgroups are in vivo phosphorylated. Plant Cell Physiol **49:** 1364–1377

Vincent D, Lapierre C, Pollet B, Cornic G, Negroni L, Zivy M (2005) Water deficits affect caffeate *O*-methyltransferase, lignification, and related enzymes in maize leaves: a proteomic investigation. Plant Physiol **137:** 949–960

Walter A, Silk WK, Schurr U (2009) Environmental effects on spatial and temporal patterns of leaf and root growth. Annu Rev Plant Biol **60:** 279–304

Wang H, Lin S, Allen JP, Williams JC, Blankert S, Laser C, Woodbury NW (2007) Protein dynamics control the kinetics of initial electron transfer in photosynthesis. Science **316:** 747–750

Welcker C, Sadok W, Dignat G, Renault M, Salvi S, Charcosset A, Tardieu F (2011) A common genetic determinism for sensitivities to soil water deficit and evaporative demand: meta-analysis of quantitative trait loci and introgression lines of maize. Plant Physiol **157:** 718–729

Wilkinson S, Davies WJ (2008) Manipulation of the apoplastic pH of intact plants mimics stomatal and growth responses to water availability and microclimatic variation. J Exp Bot **59:** 619–631

Ye Q, Steudle E (2006) Oxidative gating of water channels (aquaporins) in corn roots. Plant Cell Environ **29:** 459–470

Youssef S, Amaya I, López-Aranda J, Sesmero R, Valpuesta V, Casadoro G, Blanco-Portales R, Pliego-Alfaro F, Quesada M, Mercado J (2013) Effect of simultaneous down-regulation of pectate lyase and endo-β-1,4-glucanase genes on strawberry fruit softening. Mol Breed **31:** 313–322

Zheng Y, Zhang C, Croucher DR, Soliman MA, St-Denis N, Pasculescu A, Taylor L, Tate SA, Hardy WR, Colwill K, et al (2013) Temporal regulation of EGF signalling networks by the scaffold protein Shc1. Nature **499:** 166–171

Zhu J, Alvarez S, Marsh EL, Lenoble ME, Cho IJ, Sivaguru M, Chen S, Nguyen HT, Wu Y, Schachtman DP, et al (2007) Cell wall proteome in the maize primary root elongation zone. II. Region-specific changes in water soluble and lightly ionically bound proteins under water deficit. Plant Physiol **145:** 1533–1548